iScience, Volume *27*

Supplemental information

Coordinated metabolic responses to cyclophilin D deletion in the developing heart

Gisela Beutner, Jonathan Ryan Burris, Michael P. Collins, Chaitanya A. Kulkarni, Sergiy M. Nadtochiy, Karen L. de Mesy Bentley, Ethan D. Cohen, Paul S. Brookes, and George A. Porter Jr.

Table S1. Oligonucleotides used for PCR (related to STAR Methods).

Gene symbol	Forward Primer	Reverse Primer	Reference
18s rRNA	TAGAGGGACAAGTGGCGTTC	CGCTGAGCCAGTCAGTGT	[S1]
Atp5e	CGAAGAAGGAGTAGCTGAATCTG	CCAGGAGGTGAGGTTGATTTC	N/A
Cox8a	GGGTCCTGGATATCACCATTG	CTTCACTCCCGCTTCTTGTAG	N/A
Cox8b	GCCATAGTCGTTGGCTTCAT	CTCAGGGATGTGCAACTTCAT	N/A
Mt-CO1	GCCCCAGATATAGCATTCCC	GTTCATCCTGTTCCTGCTCC	[S1]
Myh6	CCAATGAGTACCGCGTGAAG	ACAGTCATGCCGGGATGATTG	N/A
Myh7	ATGTGCCGGACCTTGGAAG	CCTCGGGTTAGCTGAGAGAT	N/A
Ndufa1	CACTGCGTACATCCACAAATTCA	CCAGGCCCTTGGACACATA	N/A
Polr2a	GCCTCGACTTAAGGAGCTTATC	CTCGTGCAGATTGACCTAACA	[S2]
Ppif	AAAGACAGACTGGCTAGATGG	CTTCTTAGACGTCTTCCCACTT	N/A
Sdha	CTCTGAGGGATTGGCTTGATTA	AGGCTCAGCTTGCTCTTATAC	N/A
Tnni1	GAGGAAGAATGTGGAGGCTATG	CATACAGCAAGCCAACCTCTA	N/A
Tnni3	GAAGGAGGACATTGAGAAGGAAA	CATGGCTCAGCCCTCAAA	N/A
Uqcrq	CATACACCCACACCCTTAGAAC	GGTCACCACCACATGAAGAA	N/A

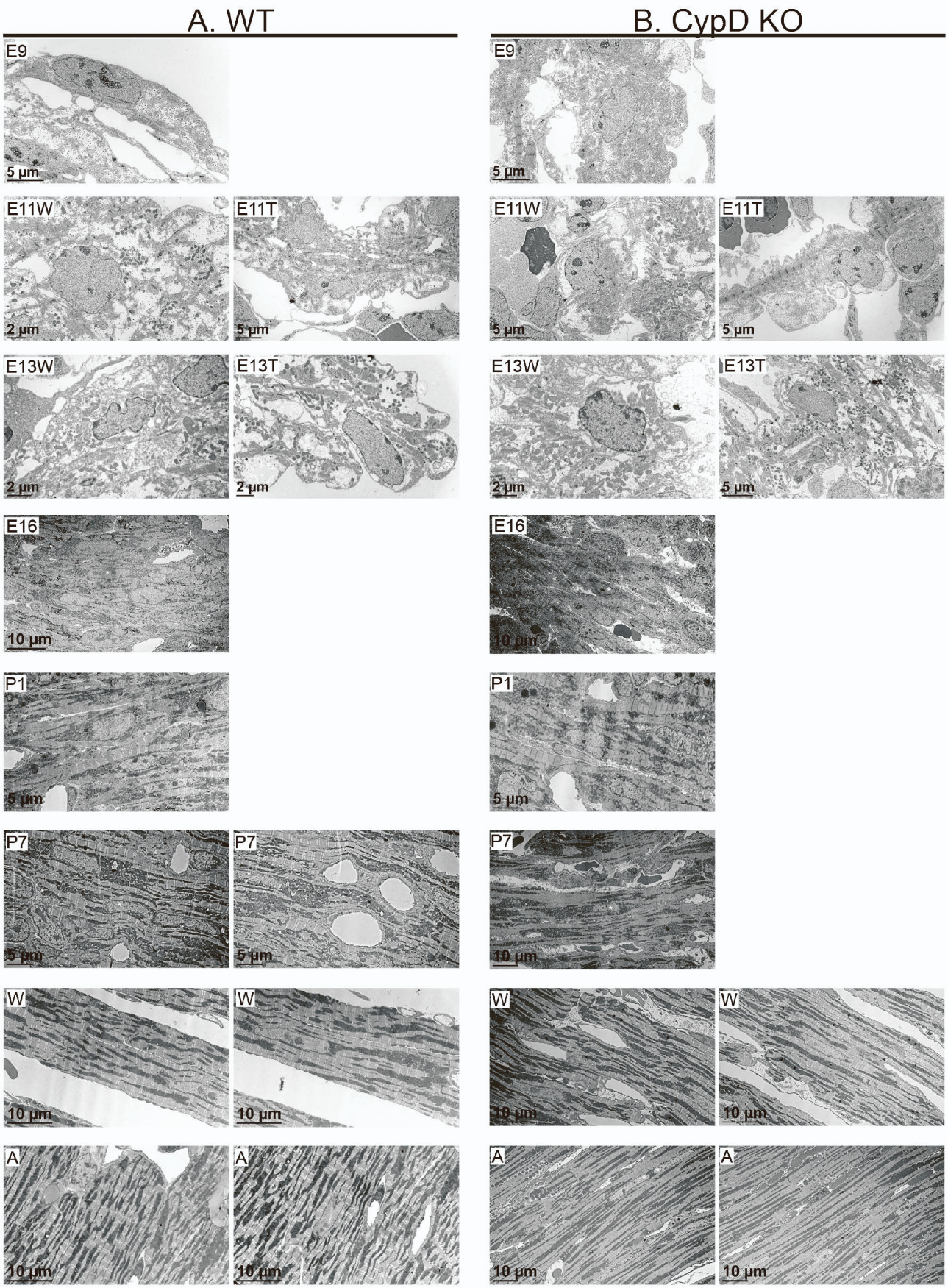

Figure S1. Additional myocyte images comparing WT and CypD KO myocytes during cardiac development (Related to Figure 1). Images of typical WT (**A**) and CypD KO (**B**) myocytes at each stage of development (E9.5, E11.5, E13.5, E16.5, P1, P7, W, A, as indicated). Note that some post-natal ages are represented by two images due to the size of the myocytes. For E11.5 and E13.5 hearts, wall (W) and trabecular (T) myocytes are presented.

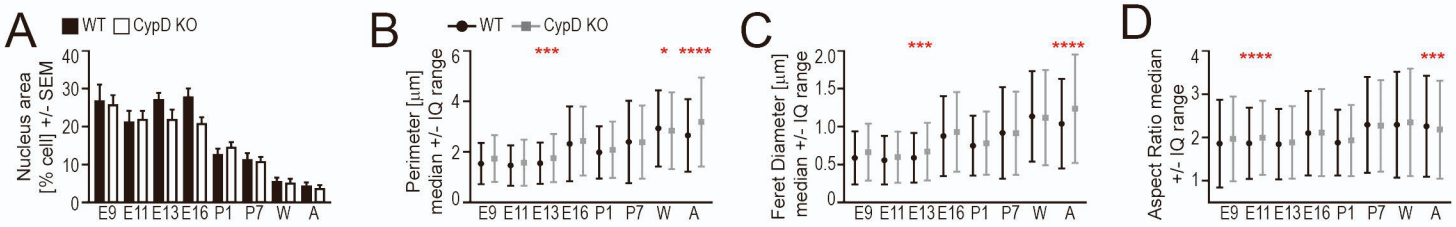

Figure S2. Additional morphometry measurements comparing WT and CypD KO myocytes during cardiac development (Related to Figure 1). (**A-D**) Morphometry was performed using low- and high-powered electron micrographs using a tablet to outline cellular structures using Fuji/Image J. Shape descriptors were copied into Excel spreadsheets and data was compiled for statistical analysis. Graphs of nuclear area as a percent of cell area (**A**) and the perimeter (**B**), Feret diameter (**C**), aspect ratio (**D**) of individual mitochondria. Data presented as Mean +/- SEM and analyzed by one-way ANOVA with Sidak's multiple comparison test (**A**) or Median +/- interquartile (IQ) range and Kruskal-Wallis with Dunn's multiple comparison test (**B-D**). Only significant comparisons between WT and CypD KO hearts at each age are shown in red stars (differences between ages of the same genotype are presented in Figure S2), *P<0.05, **P<0.01, ***P<0.001, ****P<0.0001, N=9 myocytes for **A**, N for **B-D** presented in Figure 1G).

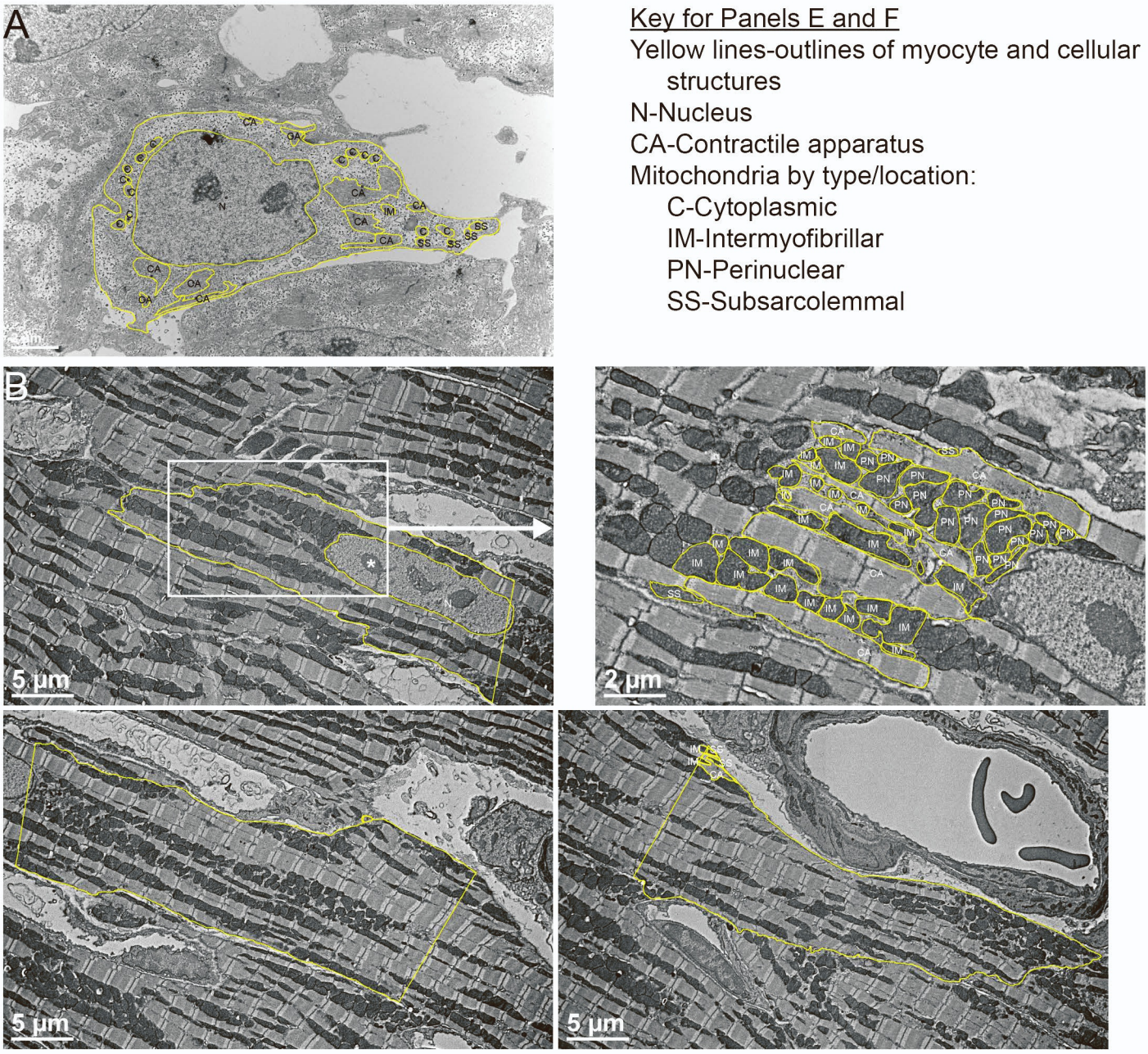

Figure S3. Examples of morphometry measurements from electron micrographs (Related to Figure 1). Lower resolution images of WT E9.5 (**A**) and Adult (**B**) myocytes from **Figure 1B** with yellow outlines of the cell, nuclei, contractile apparatus, and mitochondria subtypes (based on location) used for morphometry. Figure to the upper right in **B** is an example of a higher power image; the box in the left-hand image designates the boundaries of the right-hand image. Generally, for postnatal specimens, nuclei and cell boundaries were made on lower power images; occasionally some measurements of mitochondria and contractile apparatus structures were also made on lower power images. However, most mitochondrial and contractile apparatus images were measured using higher power images, such as the image on the right. In many cases, multiple overlapping images were used to make these measurements, and care was taken to only count specific structures once.

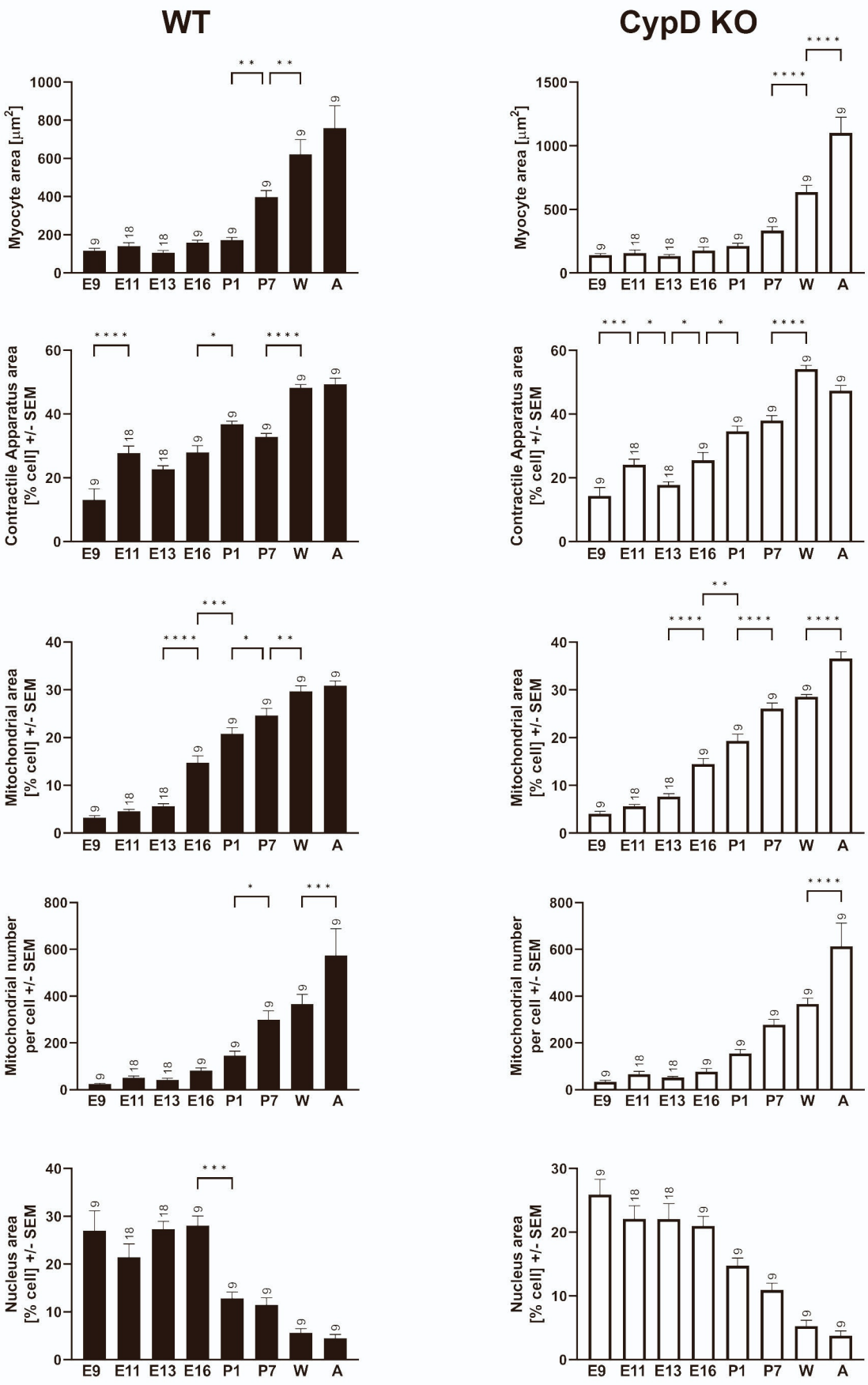

Figure S4. Additional myocyte measurements comparing WT and CypD KO cells during cardiac development (Related to Figure 1). Myocyte morphometry from electron micrographs show changes in cell size/area, contractile apparatus area, mitochondrial area, and nuclear area as a percentage of cell area, and mitochondrial number per cell at each age and genotype (WT, CypD KO), as indicated. Data is presented as Mean +/- SEM and was analyzed by one-way ANOVA with Sidek's multiple comparison test. Within each genotype (WT, CyPD KO), comparisons are made between successive ages (*P<0.05, **P<0.01, ***P<0.001, ****P<0.0001; N=9 or 18 (E11.5, E13.5) cells.

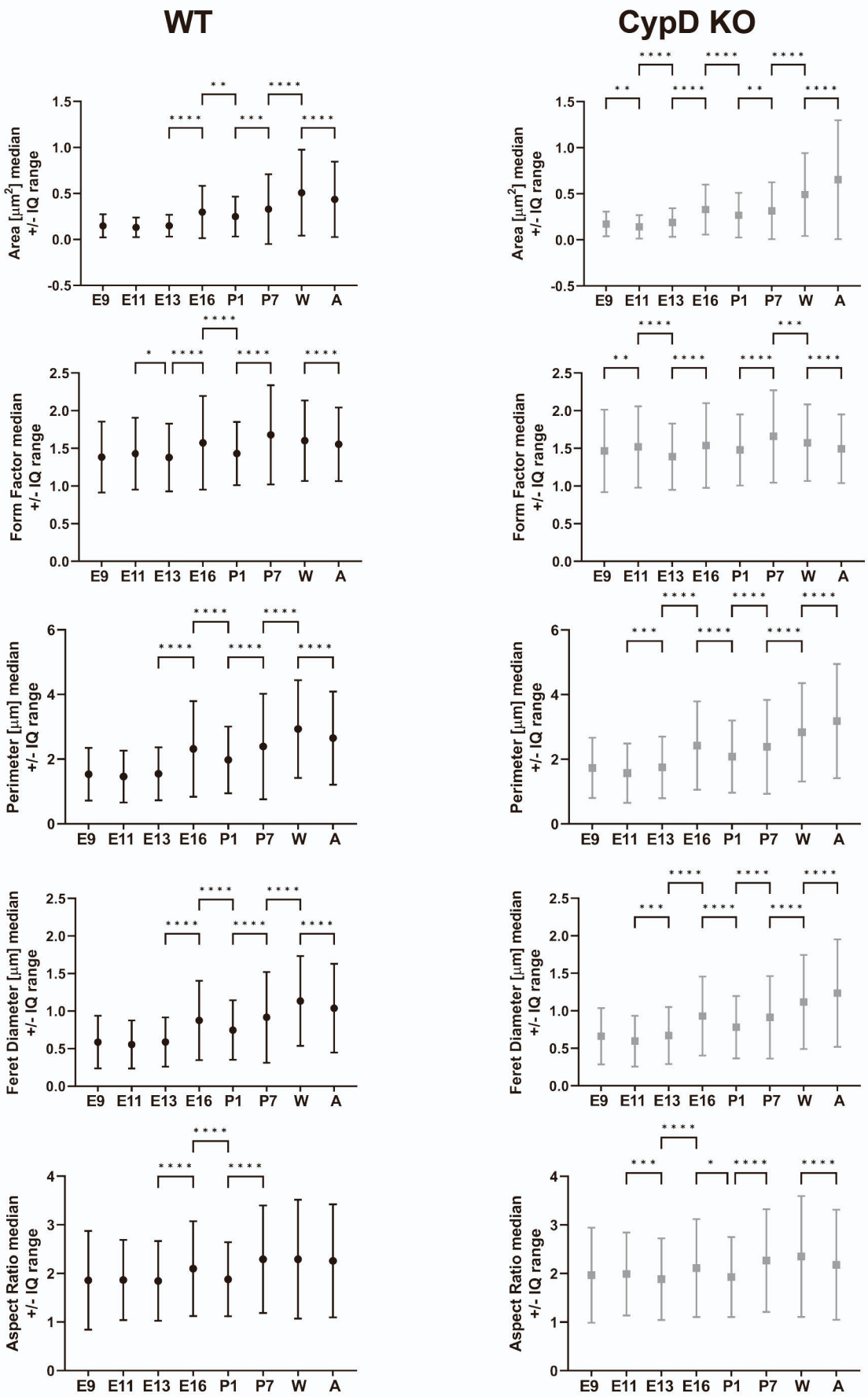

Figure S5. Additional mitochondrial morphology measurements comparing WT and CypD KO cells during cardiac development (Related to Figure 1). Morphometry of individual mitochondria show changes in mitochondrial area, perimeter, aspect ratio, form factor and Feret diameter at each age and genotype (WT, CypD KO), as indicated. Data is presented as Median +/- interquartile (IQ) range and was analyzed by Kruskal-Wallis with Dunn's multiple comparison test. Within each genotype (WT, CyPD KO), comparisons are made between successive ages (*P<0.05, **P<0.01, ***P<0.001, ****P<0.0001; N for mitochondrial shapes is indicated in Figure 1G).

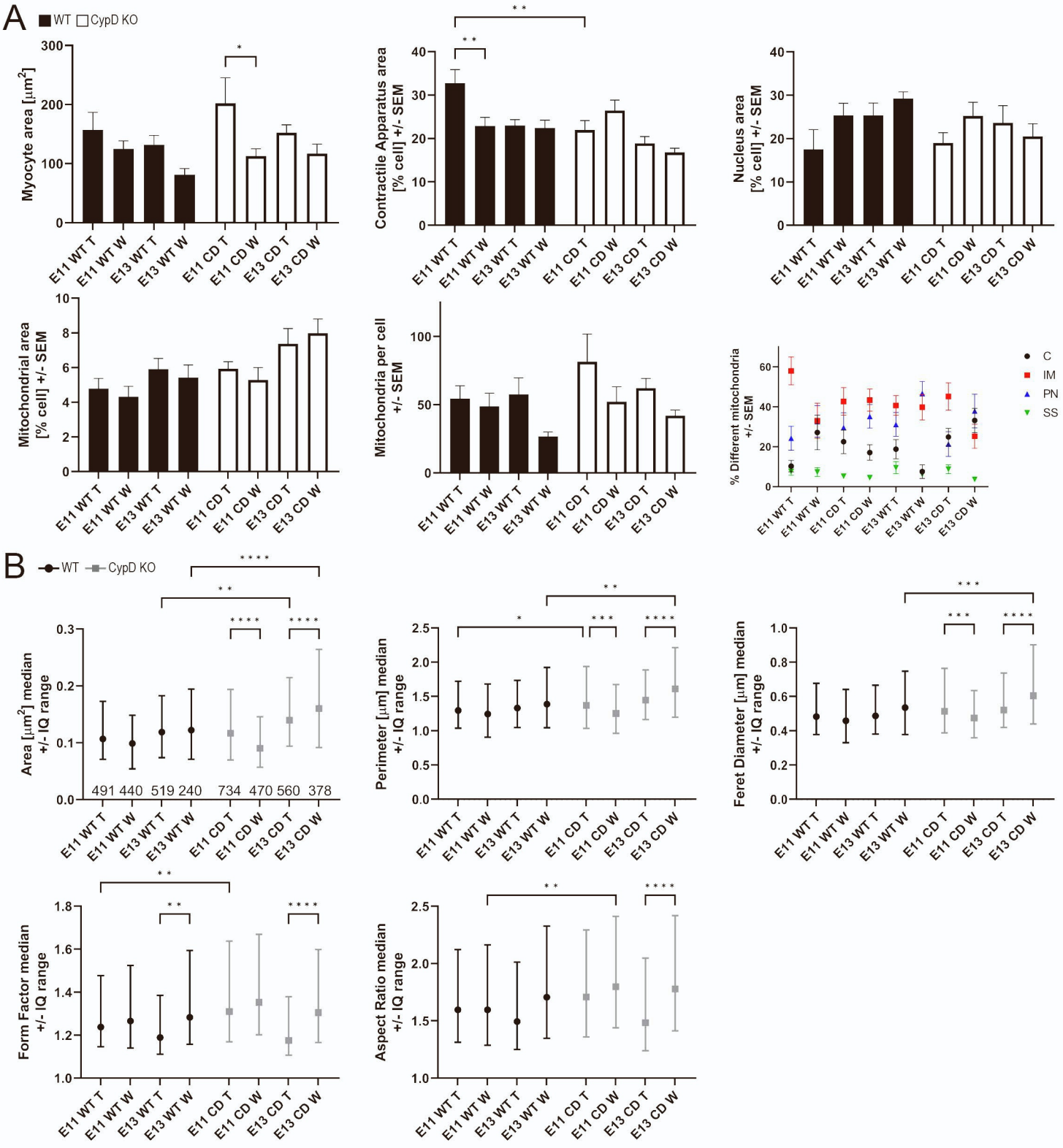

Figure S6. Subgroup analysis of WT and CypD KO cell morphometry of left ventricular myocardial wall (W) and trabecular (T) myocytes (Related to Figure 1). (**A**) Myocyte morphometry from electron micrographs show changes in cell size/area, contractile apparatus area, mitochondrial area, and nuclear area as a percentage of cell area, and mitochondrial number per cell from E11.5 and E13.5 WT and CypD KO (CD) hearts at each age, cell type (Wall or Trabeculae) and genotype (WT, CD), as indicated. Data is presented as Mean +/- SEM and analyzed by one-way ANOVA with Sidek's multiple comparison test. Percent different mitochondria in each group are also presented (lower right panel, C-cytoplasmic, IM-intermyofibrillar, PN-perinuclear, SS-subsarcolemmal). N = 9 cells per group. (**B**) Morphometry of individual mitochondria show changes in mitochondrial area, perimeter, aspect ratio, form factor and Feret diameter as in **A**. Data is presented as Median +/- interquartile (IQ) range and was analyzed by Kruskal-Wallis with Dunn's multiple comparison test, N (# of mitochondria analyzed) is presented in graph for Area. *P<0.05, **P<0.01, ***P<0.001, ****P<0.0001.

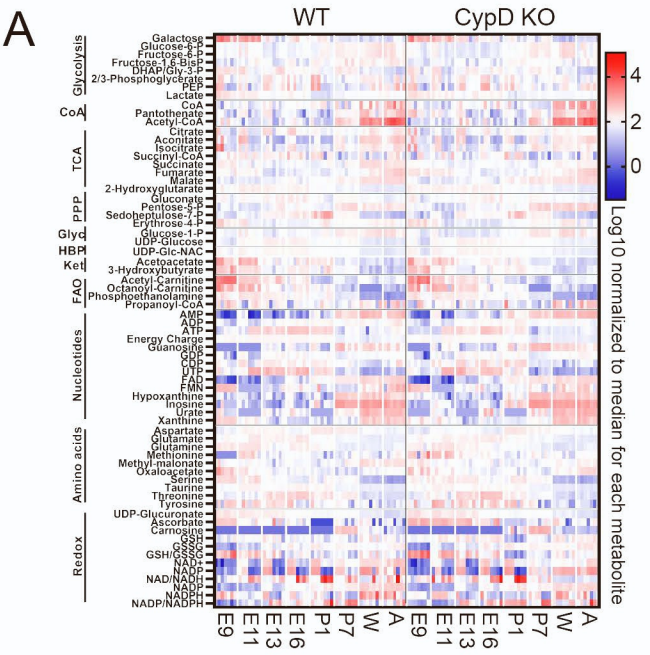

B

Component 1		Component 2	
Metabolite	Value	Metabolite	Value
FAD	-0.36	Acetyl-carnitine	+0.51
Malate	-0.35	3-Hydroxybutyrate	+0.33
AMP	-0.32	Galactose	+0.32
Inosine	-0.30	Erhthrose-4-phosphate	+0.31
2-Hydroxyglutarate	+0.29	Oxaloacetate	+0.31
Phosphoethanolamine	+0.28	Lactate	+0.31
NADP+	-0.26	UDP-glucose	-0.26
Taurine	+0.24	FMN	+0.21
Hypoxanthine	-0.23	ATP	-0.18
Pentose-5-phosphate	-0.20	Octanoyl-carnitine	+0.17
Glutamate	+0.18	Threonine	-0.15
UDP-glucuronate	+0.18	Acetoacetate	+0.11
Glutamine	+0.17	ADP	-0.09
Urate	-0.16	Isocitrate	+0.09
UDP-Glc-Nac	+0.14	Xanthine	+0.08
NADPH	-0.12	Aspartate	-0.08
Glucose-1-phosphate	-0.11	Methyl-malonate	+0.06
Serine	+0.04	GDP	-0.04
Acetyl-CoA	-0.04	GSSG	-0.03
Glucose-6-phosphate	-0.03	Aconitate	0.00

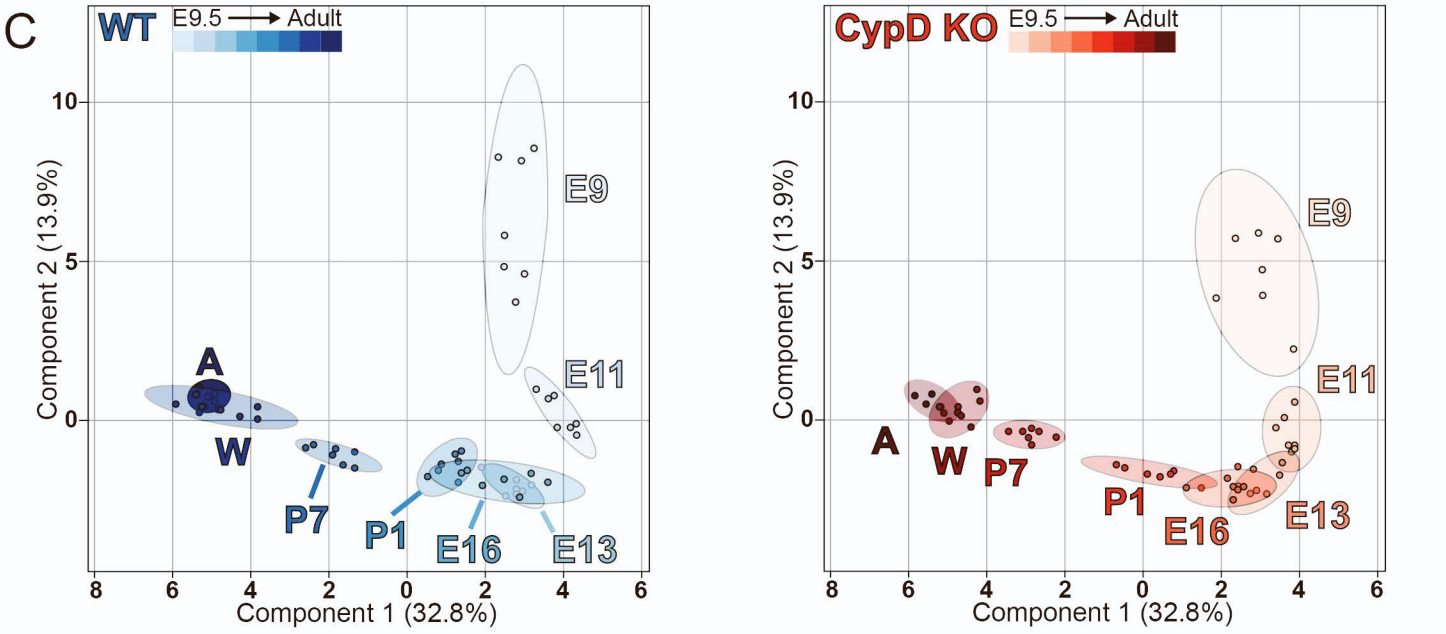

Figure S7. Additional heatmap and sPLS-DA data of metabolomic profile of WT and CypD KO hearts during development (Related to Figure 5). Sixty four metabolites were recovered by steady state, LC MS/MS metabolomics from 7 hearts at each indicated age (E9.5, E11.5, E13.5, E16.5, P1, P7, W, A) and each genotype (Wild Type, CypD KO). (**A**) Heat map of all data points for each age and genotype. Metabolites are grouped along the Y axis as metabolic pathways. (**B**) Loading for Component 1 and 2 for sparse partial least squares-discriminant analysis with the value of each metabolite from MetaboAnalyst. (**C**) Sparse partial least squares-discriminant analysis shows individual WT (left) and CypD KO (right) specimens represented as small circles and groups as larger, similarly colored ovals, while each group is marked by age. Percentage of variability explained for Components 2 and 1 are as labeled. Note that all WT and CypD KO metabolomics data was analyzed by MetaboAnalyst together, and graphs of each genotype here and in Figure 5B are presented to make data more legible.

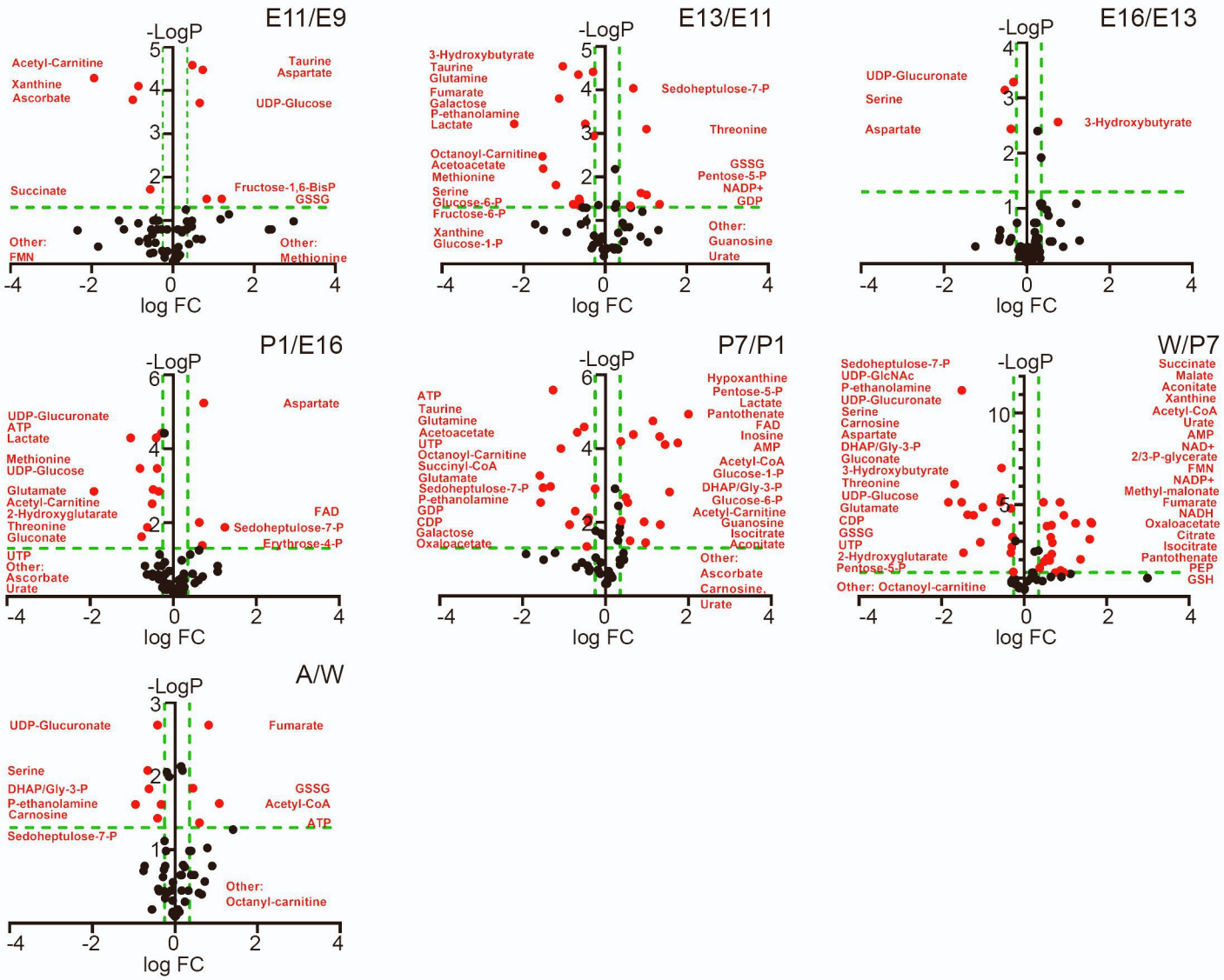

Figure S8. Additional volcano plots of metabolomic profile of WT hearts during development (Related to Figure 5). Sixty four metabolites were recovered by steady state, LC MS/MS metabolomics from 7 WT hearts at each indicated age (E9.5, E11.5, E13.5, E16.5, P1, P7, W, A). Volcano plots of metabolite changes from age to age during development reported as the -log P value versus the log FC (fold change calculated as the older age divided by the younger age) with green dashed lines demarcating a q value of 0.05 (horizontal) and FC of 0.75 and 1.5 (vertical). Significantly different metabolites are marked by red circles with their identity indicated. “Other” metabolites indicate that one group had essentially a 0 value while the other group had a measurable value.

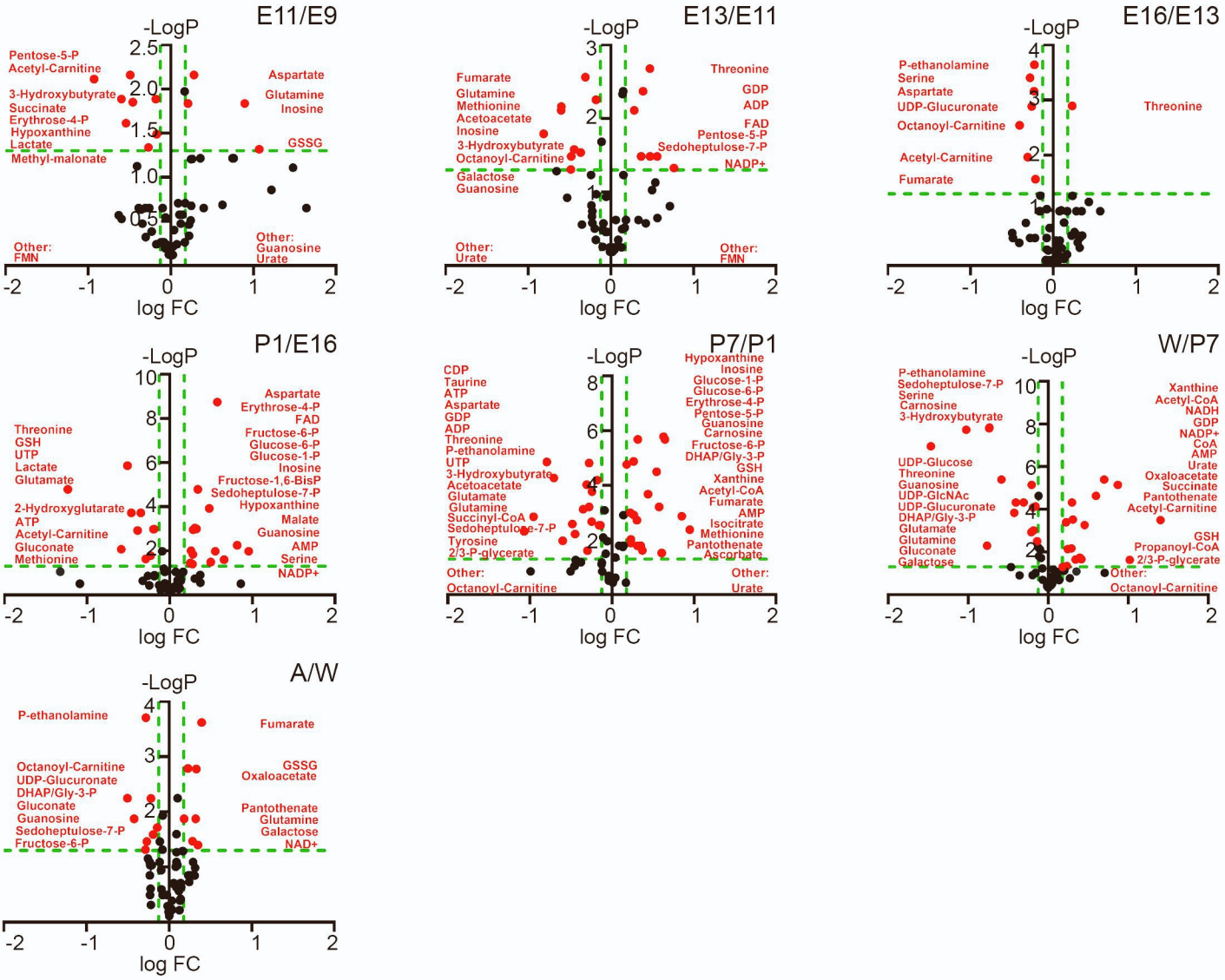

Figure S9. Additional volcano plots of metabolomic profile of CypD KO hearts during development (Related to Figure 5). Sixty four metabolites were recovered by steady state, LC MS/MS metabolomics from 7 CypD KO hearts at each indicated age (E9.5, E11.5, E13.5, E16.5, P1, P7, W, A). Volcano plots of metabolite changes from age to age during development reported as the -log P value versus the log FC (fold change calculated as the older age divided by the younger age) with green dashed lines demarcating a q value of 0.05 (horizontal) and FC of 0.75 and 1.5 (vertical). Significantly different metabolites are marked by red circles with their identity indicated. “Other” metabolites indicate that one group had essentially a 0 value while the other group had a measurable value.

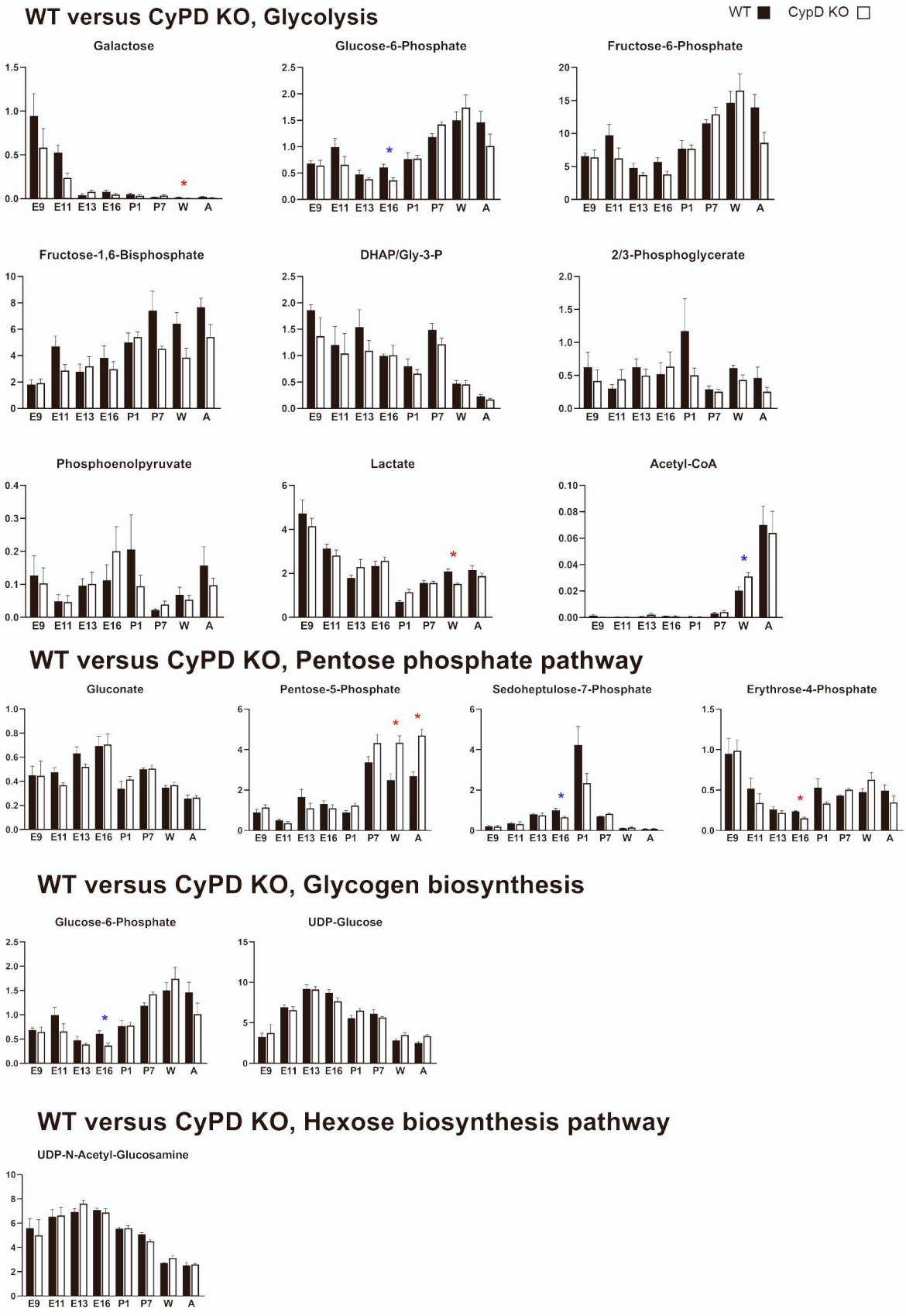

Figure S10. Column graphs of metabolites of glycolysis, pentose phosphate, glycogen biosynthesis, and hexose biosynthesis pathways from WT and CypD KO hearts during development (Related to Figure 5). Sixty four metabolites were recovered by steady state, LC MS/MS metabolomics from 7 hearts at each indicated age (E9.5, E11.5, E13.5, E16.5, P1, P7, W, A) and each genotype (Wild Type, CypD KO). Relative levels of each metabolite from each genotype represented in column graphs and grouped by metabolic pathway (note that some metabolites are represented in two pathways). Stars indicate significant differences between WT and CyPD KO hearts at that given age based on multiple T-tests using a 5% (*) or 10% (*) FDR.

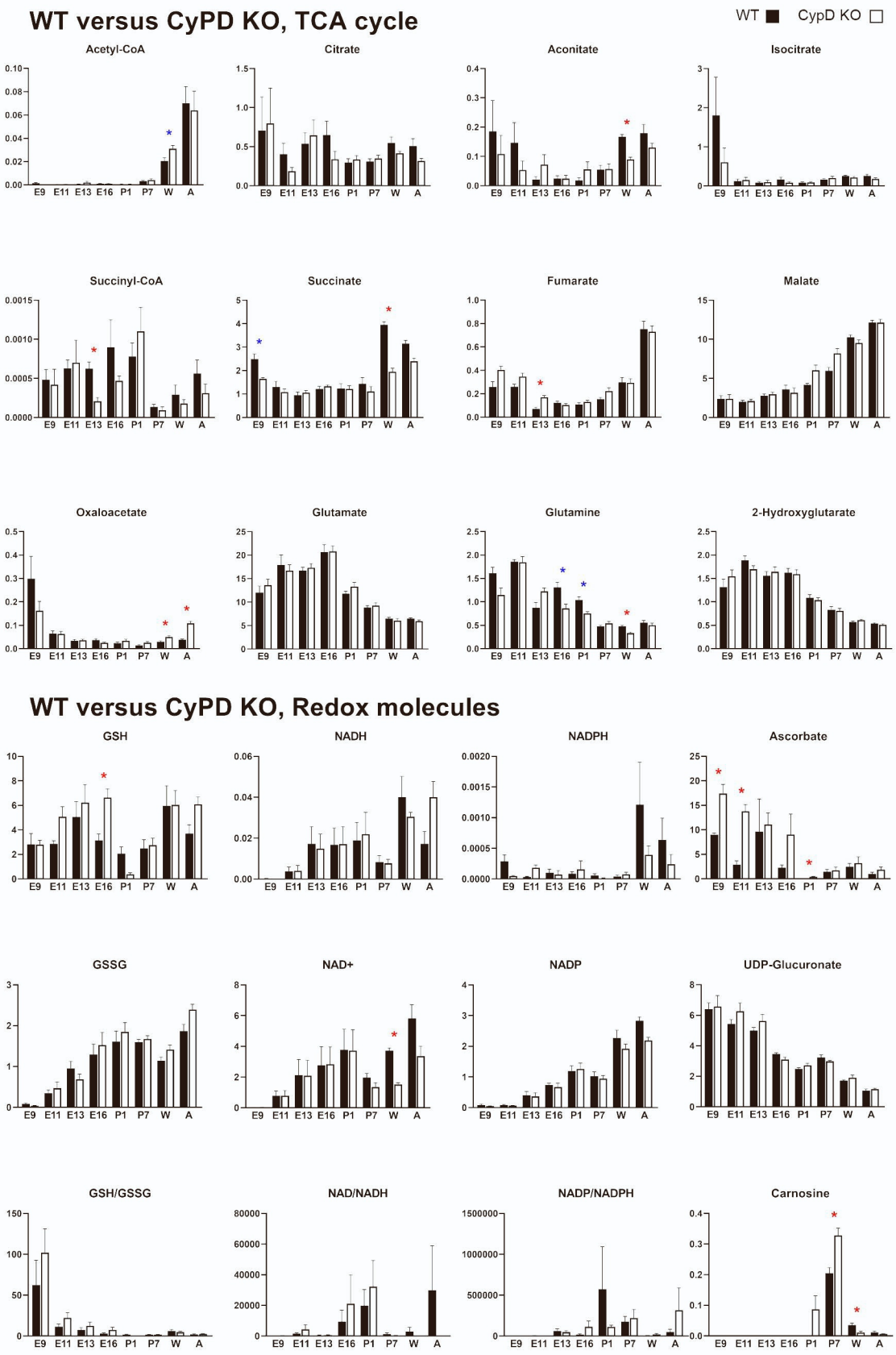

Figure S11. Column graphs of TCA cycle and Redox metabolites from WT and CypD KO hearts during development (Related to Figure 5). Sixty four metabolites were recovered by steady state, LC MS/MS metabolomics from 7 hearts at each indicated age (E9.5, E11.5, E13.5, E16.5, P1, P7, W, A) and each genotype (Wild Type, CypD KO). Relative levels of each metabolite from each genotype represented in column graphs and grouped by metabolic pathway (note that some metabolites are represented in two pathways). Stars indicate significant differences between WT and CyPD KO hearts at that given age based on multiple T-tests using a 5% (*) or 10% (*) FDR. Ratios in the bottom row are not significantly different by ANOVA.

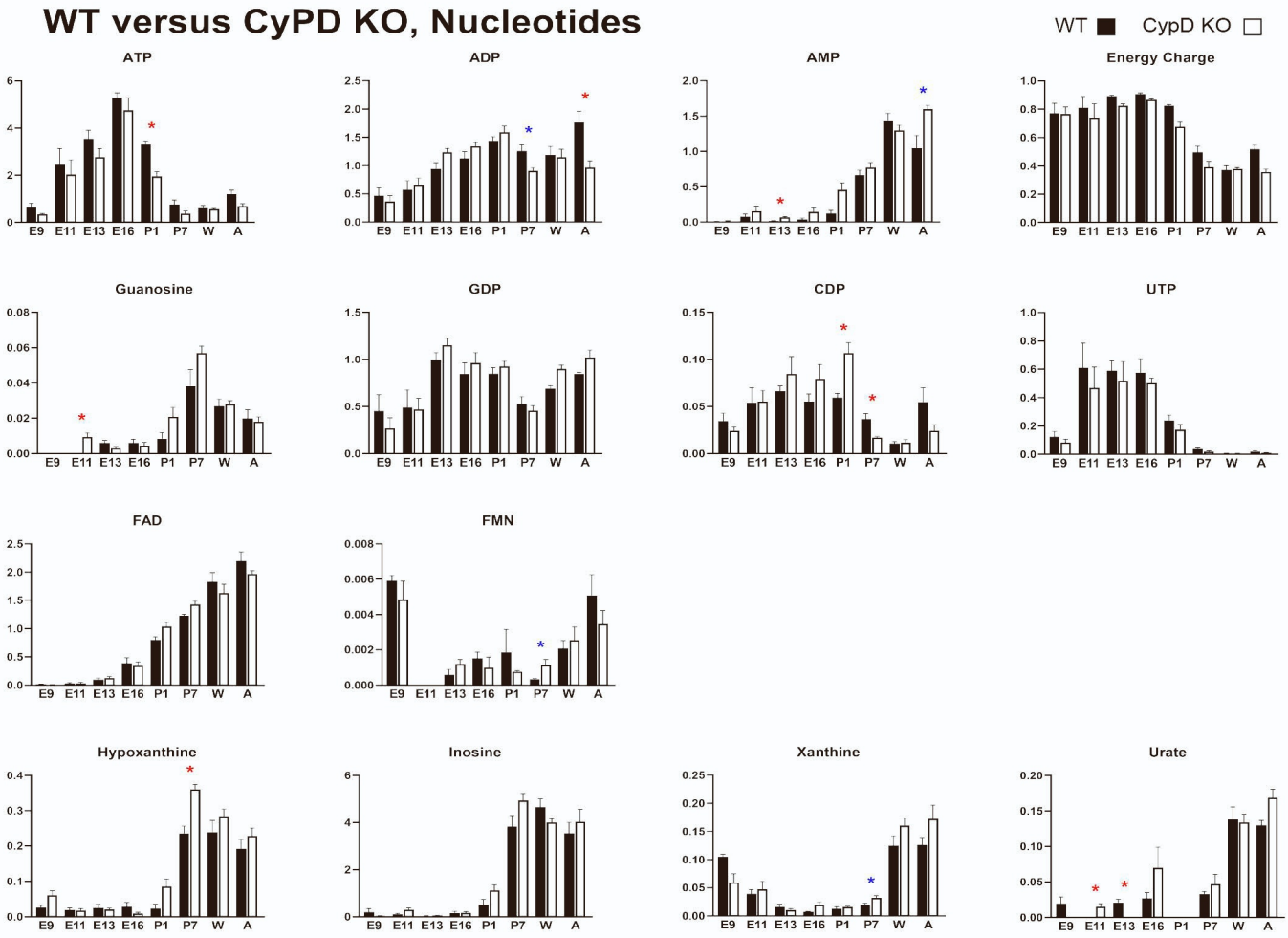

Figure S12. Column graphs of nucleotide metabolites from WT and CypD KO hearts during development (Related to Figure 5). Sixty four metabolites were recovered by steady state, LC MS/MS metabolomics from 7 hearts at each indicated age (E9.5, E11.5, E13.5, E16.5, P1, P7, W, A) and each genotype (Wild Type, CypD KO). Relative levels of each metabolite from each genotype represented in column graphs and grouped by metabolic pathway (note that some metabolites are represented in two pathways). Stars indicate significant differences between WT and CyPD KO hearts at that given age based on multiple T-tests using a 5% (*) or 10% (*) FDR. Calculated energy charge values are not significantly different by ANOVA.

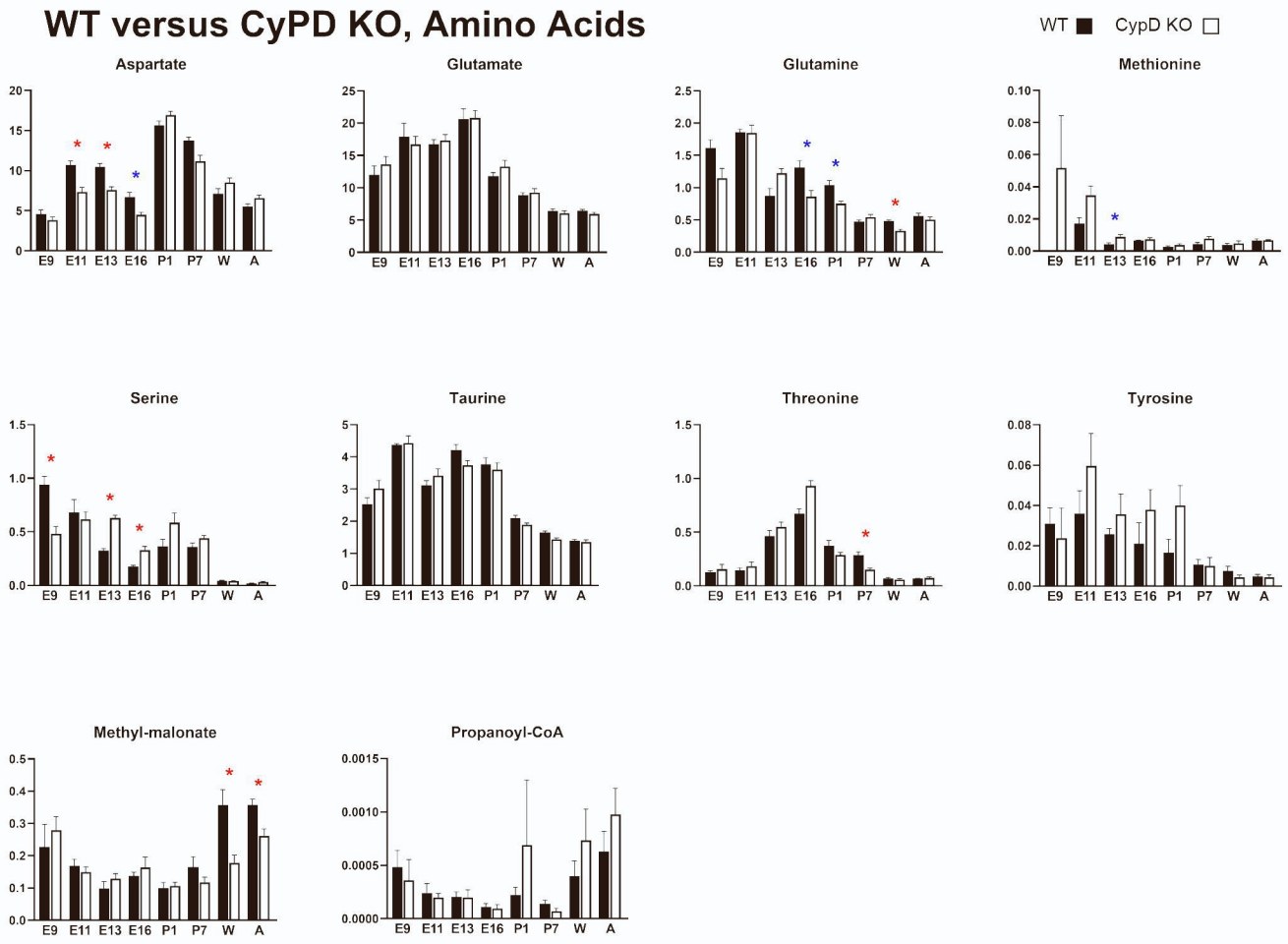

Figure S13. Column graphs of amino acid metabolites from WT and CypD KO hearts during development (Related to Figure 5). Sixty four metabolites were recovered by steady state, LC MS/MS metabolomics from 7 hearts at each indicated age (E9.5, E11.5, E13.5, E16.5, P1, P7, W, A) and each genotype (Wild Type, CypD KO). Relative levels of each metabolite from each genotype represented in column graphs and grouped by metabolic pathway (note that some metabolites are represented in two pathways). Stars indicate significant differences between WT and CyPD KO hearts at that given age based on multiple T-tests using a 5% (*) or 10% (*) FDR.

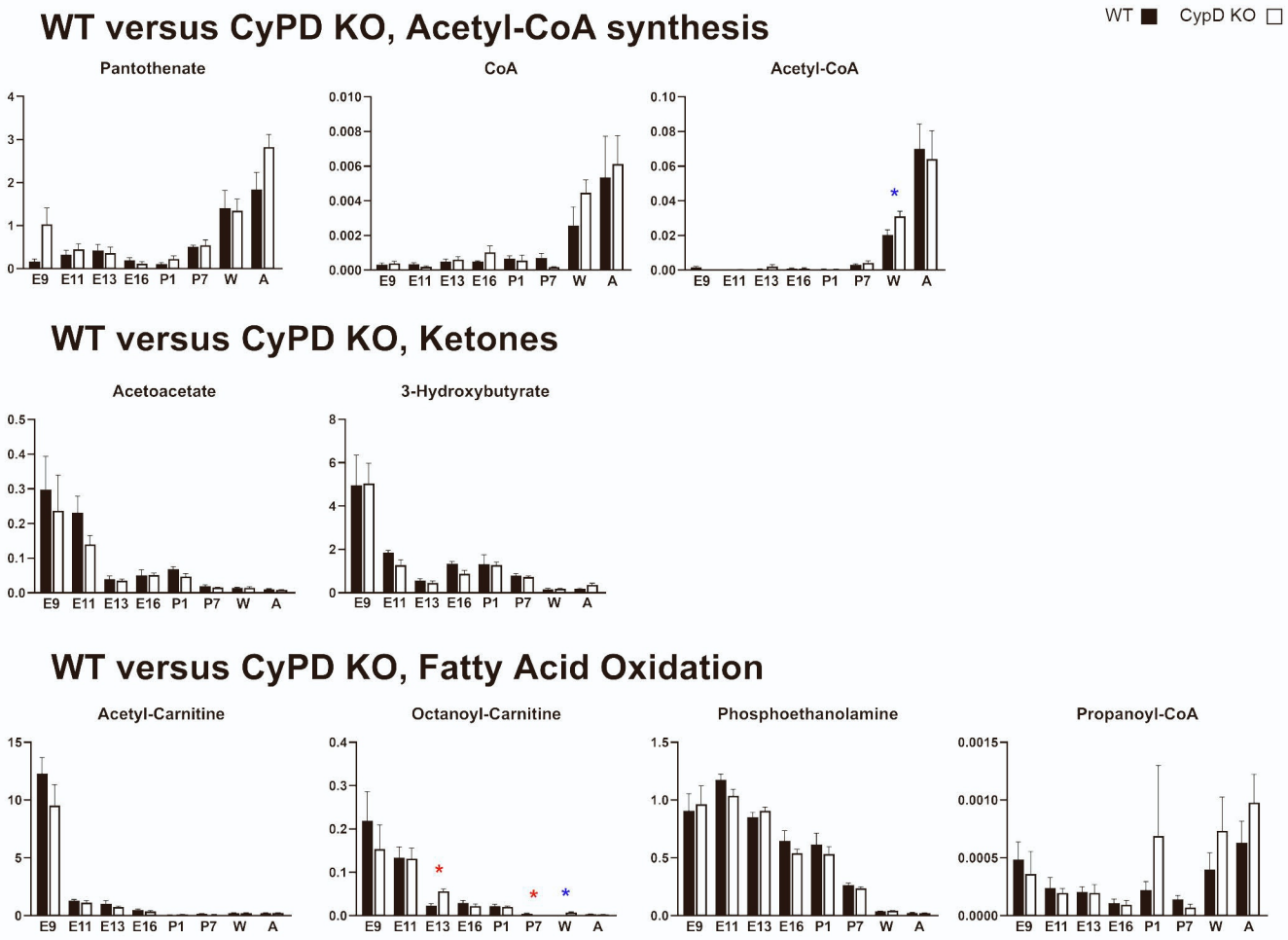

Figure S14. Column graphs of acetyl-CoA, ketone, and fatty acid oxidation metabolites from WT and CypD KO hearts during development (Related to Figure 5). Sixty four metabolites were recovered by steady state, LC MS/MS metabolomics from 7 hearts at each indicated age (E9.5, E11.5, E13.5, E16.5, P1, P7, W, A) and each genotype (Wild Type, CypD KO). Relative levels of each metabolite from each genotype represented in column graphs and grouped by metabolic pathway (note that some metabolites are represented in two pathways). Stars indicate significant differences between WT and CyPD KO hearts at that given age based on multiple T-tests using a 5% (*) or 10% (*) FDR.

SUPPLEMENTAL REFERENCES:

S1. Beutner, G., Eliseev, R.A., and Porter, G.A., Jr. (2014). Initiation of electron transport chain activity in the embryonic heart coincides with the activation of mitochondrial complex 1 and the formation of supercomplexes. PLoS One *9*, e113330. 10.1371/journal.pone.0113330.

S2. Cohen, E.D., Yee, M., Porter, G.A., Jr., Ritzer, E., McDavid, A.N., Brookes, P.S., Pryhuber, G.S., and O'Reilly, M.A. (2021). Neonatal hyperoxia inhibits proliferation and survival of atrial cardiomyocytes by suppressing fatty acid synthesis. JCI Insight *6*. 10.1172/jci.insight.140785.